

# Development of dendritic tonic GABAergic inhibition regulates excitability and plasticity in CA1 pyramidal neurons

Martine R. Groen,<sup>1</sup> Ole Paulsen,<sup>2</sup> Enrique Pérez-Garci,<sup>3</sup> Thomas Nevian,<sup>3</sup> J. Wortel,<sup>4</sup> Marinus P. Dekker,<sup>4</sup> Huibert D. Mansvelder,<sup>1</sup> Arjen van Ooyen,<sup>1\*</sup> and Rhiannon M. Meredith<sup>1\*</sup>

<sup>1</sup>Center for Neurogenomics & Cognitive Research, Department of Integrative Neurophysiology, VU University Amsterdam, Amsterdam, The Netherlands; <sup>2</sup>Department of Physiology, Development and Neuroscience, Physiological Laboratory, University of Cambridge, Cambridge, United Kingdom; <sup>3</sup>Department of Physiology, University of Berne, Berne, Switzerland; and <sup>4</sup>Center for Neurogenomics & Cognitive Research, Department of Functional Genomics, VU University Amsterdam, Amsterdam, The Netherlands

Submitted 21 January 2014; accepted in final form 18 April 2014

**Groen MR, Paulsen O, Pérez-Garci E, Nevian T, Wortel J, Dekker MP, Mansvelder HD, van Ooyen A, Meredith RM.** Development of dendritic tonic GABAergic inhibition regulates excitability and plasticity in CA1 pyramidal neurons. *J Neurophysiol* 112: 287–299, 2014. First published April 23, 2014; doi:10.1152/jn.00066.2014.—Synaptic plasticity rules change during development: while hippocampal synapses can be potentiated by a single action potential pairing protocol in young neurons, mature neurons require burst firing to induce synaptic potentiation. An essential component for spike timing-dependent plasticity is the backpropagating action potential (BAP). BAP along the dendrites can be modulated by morphology and ion channel composition, both of which change during late postnatal development. However, it is unclear whether these dendritic changes can explain the developmental changes in synaptic plasticity induction rules. Here, we show that tonic GABAergic inhibition regulates dendritic action potential backpropagation in adolescent, but not preadolescent, CA1 pyramidal neurons. These developmental changes in tonic inhibition also altered the induction threshold for spike timing-dependent plasticity in adolescent neurons. This GABAergic regulatory effect on backpropagation is restricted to distal regions of apical dendrites (>200  $\mu\text{m}$ ) and mediated by  $\alpha 5$ -containing GABA(A) receptors. Direct dendritic recordings demonstrate  $\alpha 5$ -mediated tonic GABA(A) currents in adolescent neurons which can modulate BAPs. These developmental modulations in dendritic excitability could not be explained by concurrent changes in dendritic morphology. To explain our data, model simulations propose a distally increasing or localized distal expression of dendritic  $\alpha 5$  tonic inhibition in mature neurons. Overall, our results demonstrate that dendritic integration and plasticity in more mature dendrites are significantly altered by tonic  $\alpha 5$  inhibition in a dendritic region-specific and developmentally regulated manner.

dendrite; STDP; alpha 5 GABA(A) receptor subunit; CA1 hippocampus; backpropagation

SYNAPTIC PLASTICITY, THE STRENGTHENING or weakening of synapses, occurs throughout many stages of brain development (Lohmann and Kessels 2014). In the hippocampus, the induction and expression mechanisms underlying synaptic plasticity change significantly with increasing postnatal age (Buchanan and Mellor 2007; Dudek and Bear 1993; Meredith et al. 2003; Palmer et al. 2004; Yasuda et al. 2003). Within hippocampal

rodent development, the end of the first postnatal month [postnatal days (P) 14–28] is characterized by significant changes in synaptic plasticity, from a period of hyperplasticity of excitatory synapses to a mature stable level of plasticity (Lohmann and Kessels 2014). During this period, GABAergic inhibition and dendritic morphology change significantly within the hippocampal CA1 region. However, little is known as to how these key developmental factors change signal processing in dendrites and what the functional consequences upon synaptic plasticity are.

Backpropagating action potentials (BAPs) play a critical role in spike timing-dependent synaptic plasticity (STDP) and convey information from the soma to the dendrites and spines (Campanac and Debanne 2008). BAPs are modulated by a wide range of voltage-gated ion channels, notably A-type potassium channels and h-channels (Andrasfalvy et al. 2008; Magee 1998). However, the regulation of BAPs by ligand-gated channels, such as GABA receptors, is less well studied, although GABAergic inhibition is a potent regulator of neuronal excitability (Leung and Peloquin 2006; Tsubokawa and Ross 1996) and could, therefore, affect BAPs and consequently synaptic plasticity (Andrasfalvy et al. 2008; Gasparini et al. 2007). In adult hippocampal CA1 pyramidal neurons, postsynaptic bursts of action potentials (APs) rather than single APs are necessary for STDP (Buchanan and Mellor 2007; Meredith et al. 2003; Pike et al. 1999). This higher threshold for plasticity has been hypothesized to reflect developmental differences in AP propagation into dendrites (Buchanan and Mellor 2007).

Inhibition plays a key role in neuronal signal integration and information processing (Brickley and Mody 2012; Lovett-Barron et al. 2012). In CA1 hippocampus, GABAergic inhibition is critical for hippocampal-dependent behaviors, network oscillations and synaptic plasticity (Mann and Paulsen 2007; Mody 2005; Moser et al. 2008). During postnatal development, GABAergic inhibition is upregulated and does not mature until the second postnatal month (Banks et al. 2002; Cohen et al. 2000). However, the impact of these developmental changes on BAPs and dendritic signal processing remains poorly understood.

GABAergic inhibition can act both phasically and tonically across different compartments of a CA1 pyramidal neuron. Phasic inhibition occurs at the synapse via  $\alpha 1$ – $3$ -,  $\beta$ - and  $\gamma$ -subunits at a millisecond level (Brickley and Mody 2012). In

\* A. van Ooyen and R. M. Meredith share senior authorship.

Address for reprint requests and other correspondence: R. Meredith, Center for Neurogenomics & Cognitive Research (CNCR), Dept. of Integrative Neurophysiology, VU Univ. Amsterdam, De Boelelaan 1085, Rm. C448, 1081 HV Amsterdam, The Netherlands (e-mail: r.m.meredith@vu.nl).

contrast, tonic inhibition, mediated via  $\alpha 5$ - and  $\delta$ -subunits at perisynaptic or extrasynaptic receptors, acts over seconds to minutes (Belelli et al. 2009; Brickley and Mody 2012). Whilst the effect of precisely timed phasic inhibition upon CA1 dendrites is demonstrated (Kwag and Paulsen 2009; Royer et al. 2012; Tsubokawa and Ross 1996), the effect of tonic inhibition on dendritic excitability has not been investigated. Tonic GABA(A) receptors are activated by the release of extracellular GABA by interneurons and astrocytes (Brickley and Mody 2012; Heja et al. 2012). Both cell types have spatially restricted target regions (Heja et al. 2012; Klausberger 2009). Therefore, distinct dendritic regions could be differently regulated by tonic inhibition.

Here, using a combination of somatic and dendritic electrophysiology with two-photon calcium imaging, we addressed how tonic GABAergic inhibition regulates dendritic BAPs at different preadolescent (PreAd) and adolescent (Ad) postnatal ages. We investigated the consequence for synaptic plasticity in CA1 pyramidal neurons and modeled the impact of different dendritic distributions of tonic inhibition on BAPs. Together, our results show that tonic GABAergic inhibition is mediated by  $\alpha 5$ -containing GABA(A) receptors and regulates dendritic excitability in Ad but not younger, PreAd CA1 pyramidal neurons. This effect was localized to the distal dendrites and could be explained by a distal expression pattern of dendritic  $\alpha 5$ -receptor-mediated tonic inhibition.

## MATERIALS AND METHODS

All animal use was approved by the Animal Welfare Committee of the VU University Amsterdam, according to Dutch and European law.

**Hippocampal slice preparation.** Acute horizontal hippocampal slices were obtained from 2- to 3-wk (PreAd) and 4- to 6-wk (Ad) male Wistar rats, with 2- to 3-wk (PreAd) and 4- to 7-wk old (Ad) rats used for synaptic plasticity experiments. After decapitation, the brains were rapidly dissected in 4°C slicing solution (110 mM choline chloride, 11.6 mM Na-ascorbate, 7 mM  $MgCl_2$ , 3.1 mM Na-pyruvate, 2.5 mM KCl, 1.25 mM  $NaH_2PO_4$ , 0.5 mM  $CaCl_2$ , 26 mM  $NaHCO_3$ , 10 mM glucose) (Bureau et al. 2006). Three hundred-micrometer slices were cut using a LEICA VT1000S vibratome. The slices were transferred to a slice container filled with recording artificial cerebrospinal fluid (aCSF) (125 mM NaCl, 3 mM KCl, 1.2 mM  $NaH_2PO_4$ , 2 mM  $CaCl_2$ , 1 mM  $MgSO_4$ , 26 mM  $NaHCO_3$ , 10 mM glucose). The container was heated to 35°C for 20 min after which the slices were kept at room temperature until the moment of recording, when temperature was set to 32°C.

**GABA(A) receptor pharmacology.** To address the influence of different GABA(A) subunits, we used two concentrations of gabazine (10  $\mu M$  and 200 nM) and L-655,708 (100 nM) to block both tonic and phasic inhibition, only phasic inhibition, and  $\alpha 5$  GABA(A) subunit-containing receptors, respectively (Stell and Mody 2002). To enhance tonic  $\delta$ -subunit-containing GABA(A) receptor currents, we added 4,5,6,7-tetrahydroisoxazolo[5,4-c]pyridin-3-ol (THIP; 10  $\mu M$ ) to the recording aCSF (Olmos-Serrano et al. 2010).

**Electrophysiology.** To assess the tonic and spontaneous phasic currents at the soma and in the dendrites, CA1 pyramidal cells were measured in voltage clamp mode with a high chloride intracellular solution containing K-gluconate (70 mM), KCl (70 mM), HEPES (10 mM), Mg-ATP(4 mM),  $K_2$  phosphocreatine (4 mM), GTP (0.4 mM) and biocytin (0.2%) with a pH of 7.3. In addition CGP (4  $\mu M$ ), DL-2-Amino-5-phosphonopentanoic acid (100  $\mu M$ ), and 6-cyano-7-nitroquinoxaline-2,3-dione (10  $\mu M$ ) were added to the recording aCSF to isolate GABA(A) receptor-mediated currents. To assess tonic currents, the holding current before and after gabazine application (10

$\mu M$ , 20-min wash-in period) was determined. Cells that showed a 20% or greater increase in series resistance during the recording were excluded from the analysis.

For plasticity experiments, CA1 pyramidal neurons were recorded in current clamp mode with intracellular pipette solution containing: K-gluconate (110 mM), HEPES (40 mM), NaCl (4 mM), Mg-ATP(4 mM), GTP (0.3 mM) with a pH of 7.2–7.3. Timing-dependent long-term potentiation (tLTP) was induced by patching a CA1 pyramidal neuron and stimulating an excitatory postsynaptic potential (EPSP) with an extracellular stimulation electrode placed in the Schaffer collateral pathway (50  $\mu s$ , 10–300  $\mu A$ , 0.1 Hz). After reaching a stable baseline of 12- to 15-min duration, presynaptic stimulation via the stimulation electrode was paired with a single somatic AP (5 ms pulse) at the soma via a current injection with a delay of 5 ms, repeated 30 times, a protocol shown to induce tLTP in PreAd animals (Meredith et al. 2003). Synaptic efficacy was assessed by the slope and amplitude of the induced EPSP 20 min after the pairing protocol over a 3-min period. Circa 20–25 min later, within the same cell, a second tLTP pairing was applied (5 ms pre-post delay) but with a postsynaptic AP burst (20-ms duration, 2–3 APs) instead of a single AP.

**Two-photon calcium imaging.** To assess the modulation of dendritic excitability by tonic and phasic GABA(A) inhibition during development, backpropagation of single APs and bursts of spikes was measured using two-photon calcium imaging in the presence of GABA(A) blockers. To measure dendritic excitability during normal spontaneous glutamatergic and GABAergic network activity, CA1 pyramidal neurons were patched with intracellular solution containing physiological chloride concentration (148 mM K-gluconate, 1 mM KCl, 10 mM HEPES, 4 mM Mg-ATP, 4 mM  $K_2$  phosphocreatine, 0.4 mM GTP and 0.20% biocytin, pH 7.3). The fluorescent dyes Alexa594 (80  $\mu M$ , Invitrogen) and Fluo-4 (200  $\mu M$ , Invitrogen) were added to the intracellular solution to measure morphology and calcium changes within the dendrites. After break-in, the dyes were allowed to diffuse into the dendritic tree for 20 min after which recordings started.

Either BAP(ss) (single-spike BAP) or BAP(burst) was initiated at the soma via a current injection of different amplitudes of 50-ms duration. At multiple locations along the apical shaft, BAP-induced calcium influx was assessed by the fluorescence change in Fluo-4 signal relative to the voltage insensitive Alexa594 signal (Meredith et al. 2007). Fluorescence was measured for 500-ms line scans using a LEICA RS2 two-photon laser scanning microscope with a  $\times 63$  water objective and a Ti:Sapphire laser tuned to 830-nm excitation at a bidirectional scanning frequency of 8 kHz. Three traces were averaged per distance and stimulation protocol. Amplitude, rise, and decay were extracted from the fluorescence trace by fitting a double-exponential function  $f(t) = A(e^{-t/\tau_{decay}} - e^{-t/\tau_{rise}})$ , where  $A$  is maximal amplitude and  $\tau$  is time constant. When the fit was not significantly different from baseline with a 99% confidence interval, the signal was defined as a failure, and relative amplitude change classified as zero. At the end of the experiment, a  $z$ -stack of the full dendritic tree was made, based on the Alexa594 signal. This allowed us to determine the three-dimensional trajectory from our recording site to the soma using the open source program ImageJ (Abramoff et al. 2004).

To dissect the influence of tonic and phasic currents, BAP-induced calcium transients were measured in the presence of different GABA(A) receptor-modulating drugs described above.

**Dendritic morphology reconstructions.** At the end of the experiment, the cells were fixed in 4% paraformaldehyde (PFA). Biocytin was visualized with chromogen 3,3'-diaminobenzidine tetrahydrochloride using the avidin-biotin-peroxidase method. Based on these stainings, CA1 pyramidal cell identity was confirmed. Per age group six cells were selected for manual reconstruction using NeuroLucida (MicroBrightField) with a  $\times 100$  oil objective. The morphologies of the two age groups were compared based on total dendritic length and two-dimensional Sholl analysis.

**Model simulations.** To assess the effect of the developmental increase in dendrite complexity, six reconstructed neurons per age group were imported into the NEURON simulation environment (Hines and Carnevale 1997). The model consists of passive apical and basal dendrites, with membrane capacitance  $C_m = 1 \mu\text{F}/\text{cm}^2$ , axial resistance  $R_a = 123 \Omega\text{cm}$  and passive conductance  $g_{\text{pas}} = 5 \times 10^{-5} \text{ S}/\text{cm}^2$ , as well as Hodgkin-Huxley type sodium and potassium channels at the soma, with maximal conductances  $g_{\text{Na}} = 0.07 \text{ S}/\text{cm}^2$  and  $g_{\text{K}} = 0.014 \text{ S}/\text{cm}^2$ . To assess the input resistance and capacitance, a hyperpolarizing step (300 pA) was applied at the soma. AP backpropagation into the dendrites was assessed by inserting a 20-ms depolarizing pulse at the soma (0.18–0.35 nA, depending on morphology), similar to the experiment.

To assess the effect of tonic currents in the Ad neurons, we adopted a well-established mature CA1 model that contains both active and passive properties (Poirazi et al. 2003; Sterratt et al. 2012). We distributed tonic inhibitory conductances (Pavlov et al. 2009) in the apical dendrite according to five different expression profiles: distally increasing, distally decreasing, localized, uniform and no tonic conductances at all. Maximum conductance ( $g_{\text{max}}$ ) depended on path distance from the soma with a minimum of  $0 \mu\text{S}$  and a maximum of  $0.030 \mu\text{S}$ . In the localized expression profile, tonic conductances ( $0.030 \mu\text{S}$ ) were only inserted in dendritic compartments that were 200–400  $\mu\text{m}$  from soma. In the uniform expression profile, tonic  $g_{\text{max}}$  was set to  $0.015 \mu\text{S}$  for all dendritic compartments. Simulation code will be made publicly available in ModelDB (<http://senselab.med.yale.edu/modeldb>).

**Electron microscopy.** PreAd (P14) and Ad (P28) male Wistar rats ( $n = 4$  for both age groups) were deeply anesthetized by isoflurane (2%), followed by an intraperitoneal injection of urethane (1.79 g/kg). Brains were fixed by transcardial perfusion with 0.9% NaCl, followed by PFA fixative (4% PFA, 2.5% glutaraldehyde dissolved in 0.1 M phosphate-buffered saline, pH 7.4). Horizontal hippocampal slices of 50  $\mu\text{m}$  were postfixed in 1%  $\text{OsO}_4$  and stained with 1% ruthenium. After embedding in Epon, ultrathin sections ( $\sim 90 \text{ nm}$ ) were collected on 400-mesh copper grids, followed by staining with ruthenium (1%) and lead citrate. Digital images of symmetric (GABAergic) and asymmetric (glutamatergic) synapses were taken at  $\times 100,000$  magnification using a Jeol (Peabody, MA) 1010 electron microscope.

Only synapses which showed clear post- and presynaptic properties were selected for analysis. For each synapse, the postsynaptic density (PSD) length and cluster size, number of docked vesicles and number of undocked vesicles were determined. Cluster size is defined as the area within the presynaptic terminal that contains synaptic vesicles, both docked and undocked. A vesicle was classified as docked when there was no separation detectable between the presynaptic membrane and the vesicle membrane. The observer was unaware of the age group while counting.

**Statistical methods.** When comparing multiple datasets, an ANOVA followed by post hoc test with a Bonferroni correction was performed. For a comparison between two datasets, a *t*-test was performed. Differences were regarded as significant when the *P* value was below 0.05 (\* $P < 0.05$ , \*\* $P < 0.01$ , \*\*\* $P < 0.001$  in Figs. 1–9).

## RESULTS

Induction rules for STDP in the hippocampus differ significantly with increasing postnatal age (Buchanan and Mellor 2007; Meredith et al. 2003). Comparing rodent hippocampal slices taken from a period of preadolescence (P14–19) with adolescence (P28–42), we measured the level of tLTP between Schaffer collateral synapses on to CA1 pyramidal neurons (Fig. 1A). Using two different induction paradigms, we observed a significantly higher level of tLTP induced by a pairing protocol with single postsynaptic APs [single-spike (SS) pairing] in PreAd com-

pared with Ad neurons (SS pairing, Fig. 1B, PreAd:  $101 \pm 26\%$ ,  $n = 11$  vs Ad:  $32 \pm 14\%$ ,  $n = 11$ , independent samples *t*-test  $P = 0.030$ ). Following additional pairing with postsynaptic bursts of APs (BS pairing), synaptic strength significantly increased in Ad neurons (Ad:  $99 \pm 18\%$ ) to a level that was similar to PreAd neurons (BS pairing, Fig. 1A, PreAd:  $127 \pm 44\%$ , independent samples *t*-test  $P = 0.54$ ).

Given the difference in postsynaptic AP requirements for plasticity, we tested whether backpropagation of single APs and bursts of spikes differed in PreAd and Ad dendrites using two-photon calcium imaging. Backpropagation was determined as a change in the fluorescence of the calcium-sensitive dye, Fluo-4, as measured with two-photon calcium imaging at different distances from the soma (Fig. 1B, see MATERIALS AND METHODS). There were significant differences in the level of backpropagation for single APs and bursts across age groups [ANOVA  $F_{(3,38)} = 10.4$ ,  $P < 0.001$ ]. Single BAPs were detected at significantly greater distances along dendrites from PreAd compared with Ad neurons [PreAd:  $408 \pm 56 \mu\text{m}$  ( $n = 7$ ), Ad:  $221 \pm 27 \mu\text{m}$  ( $n = 16$ ), post hoc *t*-test,  $P < 0.01$ , Fig. 1C]. There was no significant change in propagation distance of single APs vs. bursts of spikes in younger neurons [BS values PreAd:  $488 \pm 46 \mu\text{m}$  ( $n = 8$ )  $P = 1$ , nonsignificant, Fig. 1C], but in Ad dendrites, there was a trend for bursts of spikes to propagate significantly further than single APs [SS:  $221 \pm 27 \mu\text{m}$  ( $n = 16$ ), BS:  $358 \pm 34 \mu\text{m}$  ( $n = 8$ ),  $P = 0.066$ ] to a distance similar to that seen with bursts in PreAd dendrites ( $P = 0.21$ , Fig. 1C). Thus dendritic excitability in response to backpropagation of single APs and bursts is significantly altered between PreAd and Ad developmental stages.

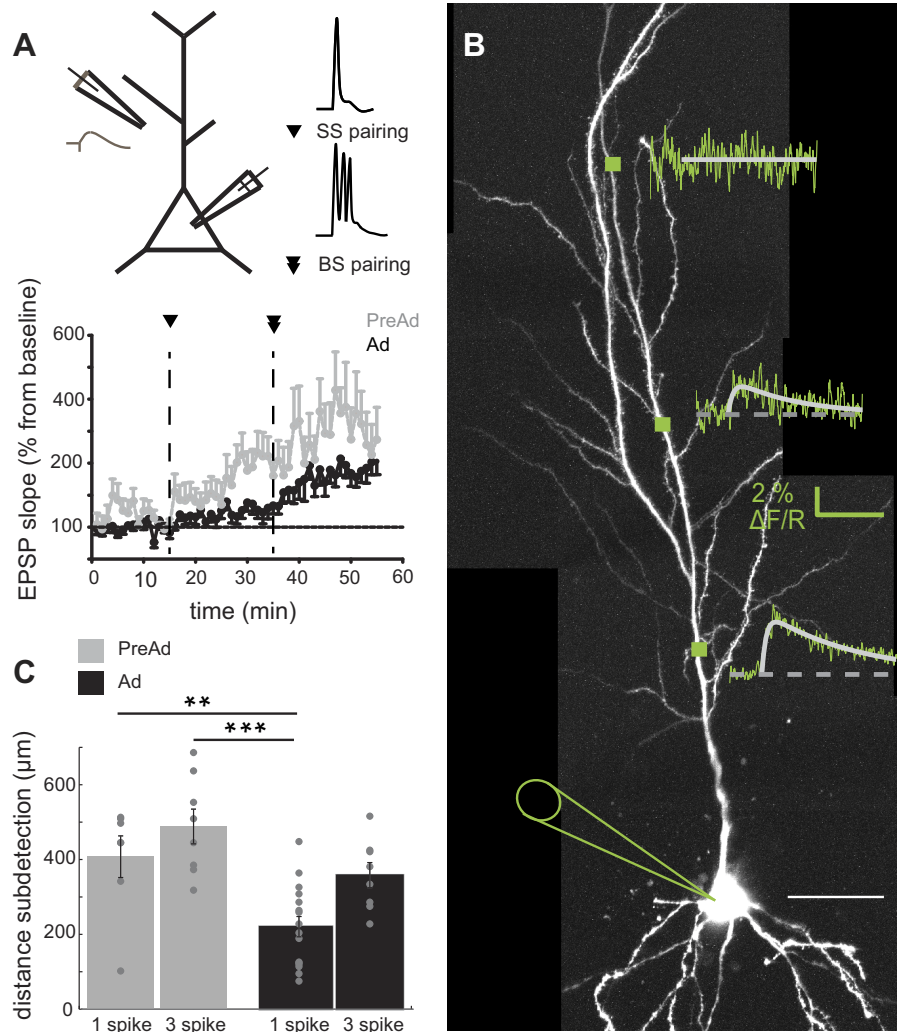
During hippocampal development, CA1 pyramidal neurons undergo prominent changes in both their neuronal morphology and regulation by GABAergic inhibition. To determine whether either of these mechanisms could underlie the change in tLTP induction rules observed, we first characterized the maturation of dendritic and both excitatory and inhibitory synaptic morphology during the same developmental period (Fig. 2). For both age groups, dendritic morphology of six CA1 pyramidal cells was reconstructed. Total dendritic length of both apical and basal dendrites significantly increased during development [Fig. 2, A and B, apical PreAd  $5.7 \pm 0.4 \text{ mm}$  ( $n = 6$ ), Ad  $7.7 \pm 0.2 \text{ mm}$  ( $n = 6$ ),  $P = 0.0017$ ; basal PreAd  $1.7 \pm 0.2$  ( $n = 6$ ), Ad  $3.1 \pm 0.2 \text{ mm}$  ( $n = 6$ ),  $P = 0.0011$ ]. Sholl analysis revealed an increased number of basal and thin oblique dendrites at 200–275  $\mu\text{m}$  in older neurons compared with PreAd neurons (Fig. 2, C and D).

At the ultrastructural level, GABAergic pre- and postsynaptic properties were quantified at the electron microscopy level in two dendritic regions, stratum radiatum (SR) and stratum lacunosum moleculare (SLM) (Fig. 2, E and G). Glutamatergic synapses have asymmetric profiles with a thick strongly labeled PSD, while GABAergic synapses have a symmetric profile with a thin PSD (Fig. 2, E and G) (Lund et al. 2001; Marty et al. 2002; Megias et al. 2001).

The number of docked vesicles in GABAergic synapses showed a prominent increase with age in both SR and SLM [Fig. 2H, middle, SR PreAd  $2.77 \pm 0.11$  ( $n = 108$ ), Ad  $3.97 \pm 0.14$  ( $n = 120$ ),  $P < 0.001$ ; SLM PreAd  $2.54 \pm 0.10$  ( $n = 114$ ), Ad  $4.54 \pm 0.19$  ( $n = 114$ ),  $P < 0.001$ ]. In the Ad group, this upregulation in number of docked vesicles was significantly greater in SLM than in SR [Fig. 2H, middle, SR  $3.97 \pm$



Fig. 1. Hippocampal spike timing-dependent synaptic plasticity (STDP) rules change with developmental age. *A, top*: experimental paradigm for timing-dependent long-term potentiation (LTP) induced in CA1 pyramidal cells. During pairing protocols, each cell was stimulated with a single action potential (SS) 12–15 min after a stable baseline and 20–25 min later, followed by a subsequent postsynaptic burst (BS) of action potentials. *Bottom*: change in excitatory postsynaptic potential (EPSP) slope following single-spike (SS) and burst (BS) pairing protocols for neurons from preadolescent (PreAd) [postnatal days (P) 14–19] and adolescent (Ad) (P28–42) brain slices in artificial cerebrospinal fluid (aCSF). *B*: CA1 pyramidal neuron filled with Alexa594 and Fluo-4 dyes overlaid with corresponding calcium transients as determined by line scans across apical dendritic regions at marked locations corresponding to distance-dependent backpropagating action potential (BAP). A double exponential was fitted to the calcium transient to determine peak, rise and decay. Scale bar 50  $\mu\text{m}$ . *C*: distance measured along the dendrite at which it was not possible to detect a suprathreshold calcium transient in response to single or bursts of action potentials in PreAd and Ad neurons. Post hoc *t*-test value:  $**P < 0.01$ ,  $***P < 0.001$ .



0.14 ( $n = 120$ ), SLM  $4.54 \pm 0.19$  ( $n = 114$ ),  $P = 0.015$ ]. Similarly, the number of undocked vesicles in SLM also increased during this developmental period, indicating a total increase in vesicle number [Fig. 2H, right, PreAd  $40.1 \pm 2.9$  ( $n = 114$ ), Ad  $53.1 \pm 2.8$  ( $n = 114$ ),  $P = 0.0016$ ]. Cluster size (data not shown) and active zone length of GABAergic synapses showed near mature levels at P14, with only a small increase in active zone length in SR [Fig. 2H, left, PSD SR PreAd  $336 \pm 10$  nm ( $n = 108$ ), Ad  $374 \pm 11$  nm ( $n = 120$ ),  $P = 0.015$ ].

In contrast to GABAergic synapses, glutamatergic synapses did not change significantly in any ultrastructural properties measured between these periods, except for an increase in the number of undocked vesicles in SLM region synapses [Fig. 2F, PreAd:  $30.2 \pm 1.9$  ( $n = 125$ ), Ad:  $37.2 \pm 2.4$  ( $n = 116$ ),  $P = 0.024$ ]. Together, these data show that morphology of both dendrites and GABAergic synapses on CA1 pyramidal neurons undergoes significant maturation during this postnatal developmental period.

Neuronal morphology can prominently alter dendritic excitability and AP backpropagation (Golding et al. 2001; van Elburg and van Ooyen 2010; Vetter et al. 2001; Yang et al. 2012). In addition, dendrite diameter has significant effects on input resistance and voltage (Migliore et al.

2005). To isolate the effect of morphological changes, we assessed passive neuronal properties and dendritic backpropagation in a simplified passive NEURON model, in which morphology parameters were varied based upon the reconstructed morphologies of CA1 pyramidal neurons (Fig. 2). All models contained the same active Hodgkin-Huxley-like channels in the soma, passive leak channels in dendrites and were stimulated with hyperpolarizing and depolarizing steps at the soma, similar to the experiments with real neurons. There was a clear developmental decrease in input resistance [Fig. 3B, top, PreAd  $144 \pm 11$  ( $n = 6$ ), Ad  $108 \pm 11$  M $\Omega$  ( $n = 6$ ),  $P = 0.040$ ], but no significant effect on membrane time constants [Fig. 3B, bottom, PreAd  $20.1 \pm 0.2$  ( $n = 6$ ), Ad  $20.1 \pm 0.1$  ms ( $n = 6$ ),  $P = 0.97$ ]. This pattern replicated the experimental data [Fig. 3A, input resistance PreAd  $182 \pm 12$  ( $n = 6$ ), Ad  $126 \pm 15$  M $\Omega$  ( $n = 6$ ),  $P = 0.014$ ;  $\tau$  PreAd  $31.0 \pm 3.6$  ( $n = 6$ ), Ad  $27.5 \pm 2.7$  ms ( $n = 6$ ),  $P = 0.47$ ], showing that the increased morphological complexity observed during development resulted in a lower input resistance. However, backpropagation into distal dendritic regions, indicated by peak voltage of BAP, was not affected by morphological differences [Fig. 3, C and D, exponential decay PreAd  $329 \pm 67$   $\mu\text{m}$  ( $n = 6$ ), Ad  $331 \pm 30$   $\mu\text{m}$  ( $n = 6$ ),  $P = 0.98$ ]. Thus developmental changes in morphology can explain maturation

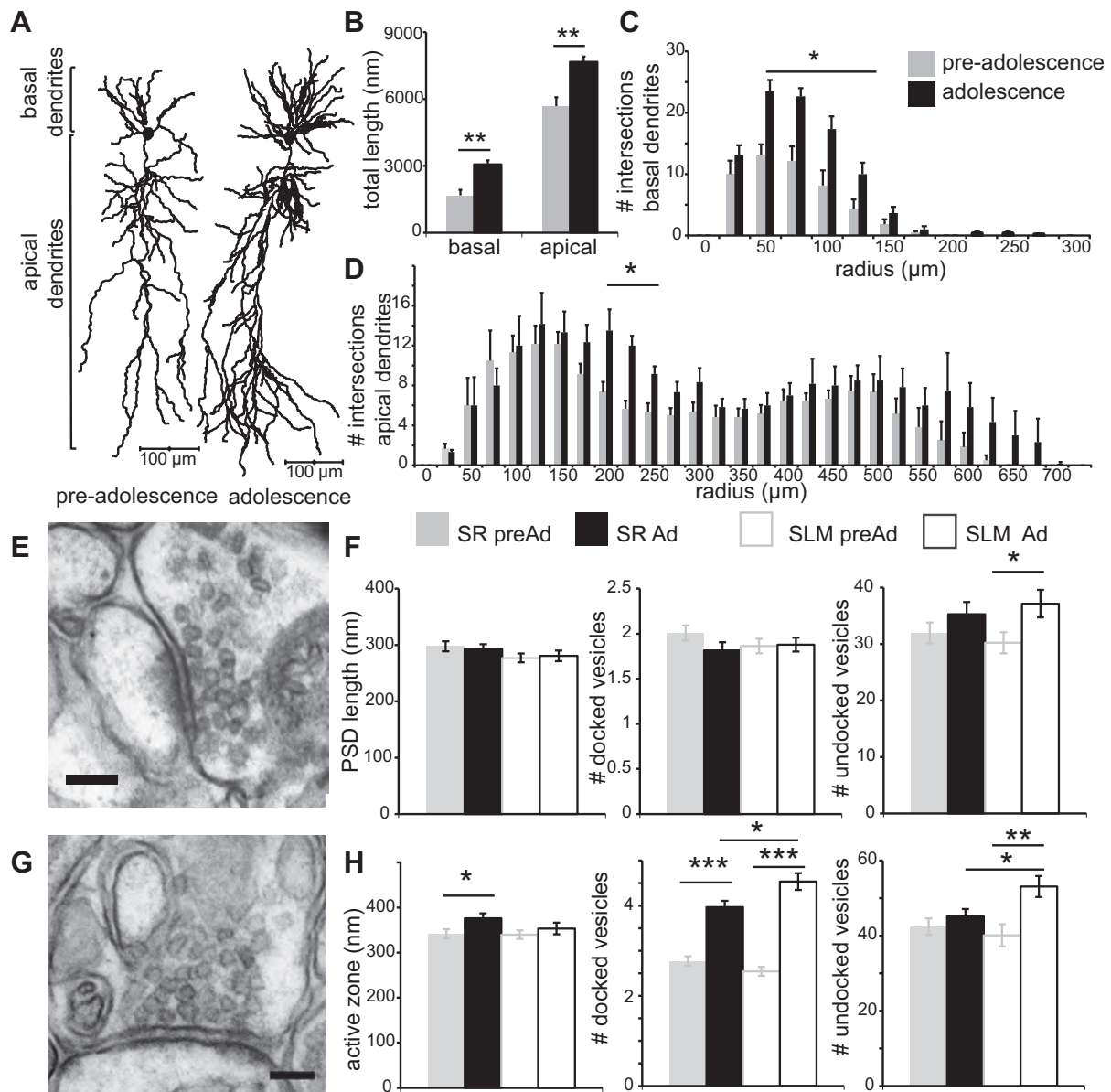


Fig. 2. CA1 pyramidal neurons undergo significant dendritic and synaptic morphology changes from PreAd to Ad stages. **A**: example reconstructions of two biocytin-filled neurons from P14–19 and P28–46 age groups. **B**: total dendritic length is significantly increased in older neurons in basal and apical dendrites. **C** and **D**: significant increase in numbers of intersections for basal and apical dendrites of Ad neurons (Sholl analysis). **E** and **G**: representative examples of electron microscopy images of stratum radiatum (SR; *top*) and stratum lacunosum moleculare (SLM; *bottom*) GABAergic synapse. Note the sparsely labeled postsynaptic density (PSD), creating a symmetric synapse appearance, characteristic for GABAergic synapses. Scale bar indicates 100 nm. **F**: PSD length and docked and undocked vesicle counts for glutamatergic synapses. **H**: active zone is significantly increased during development in SR synapses. There was a significant developmental increase of number of docked vesicles in both regions. There was a significant developmental increase of number of undocked vesicles in SLM. In addition, Ad SLM synapses contained more vesicles than Ad SR synapses. \* $P < 0.05$ . \*\* $P < 0.01$ . \*\*\* $P < 0.001$ .

of neuronal passive properties but do not significantly alter distance-dependent backpropagation into distal dendrites.

Dendritic BAP is necessary for induction of STDP (Feldman 2012; Kampa et al. 2007). An increase in GABAergic inhibition onto dendrites, as observed during the Ad stage (Fig. 2; Banks et al. 2002; Cohen et al. 2000), is predicted to decrease excitability of neurons and to modulate dendritic BAP. To investigate the functional consequences of increased GABAergic inhibition upon STDP, tLTP induction paradigms were tested in Ad neurons in the presence of the GABA(A) receptor antagonist, gabazine (Fig. 4). The contributions of tonic and phasic inhibition were separated

using differing concentrations of gabazine (Stell and Mody 2002). Blocking phasic but leaving tonic inhibition intact, Ad neurons still required BS for tLTP, similar to control aCSF conditions [Fig. 4, **A** and **C**, 200 nM gabazine: single AP (SS) pairing:  $124 \pm 19\%$  ( $n = 5$ ),  $P = 0.28$  from baseline, burst (BS) pairing:  $180 \pm 7\%$  EPSP slope potentiation ( $n = 5$ ),  $P < 0.001$ ]. However, blocking both tonic and phasic inhibition with a higher gabazine concentration lowered the threshold for tLTP to that of PreAd neurons [Fig. 4, **B** and **C**, 10  $\mu$ M gabazine: single AP (SS) pairing:  $132 \pm 14\%$ ,  $n = 11$ , burst (BS) pairing:  $199 \pm 18\%$  EPSP slope potentiation,  $n = 11$ ,  $P < 0.001$ ].

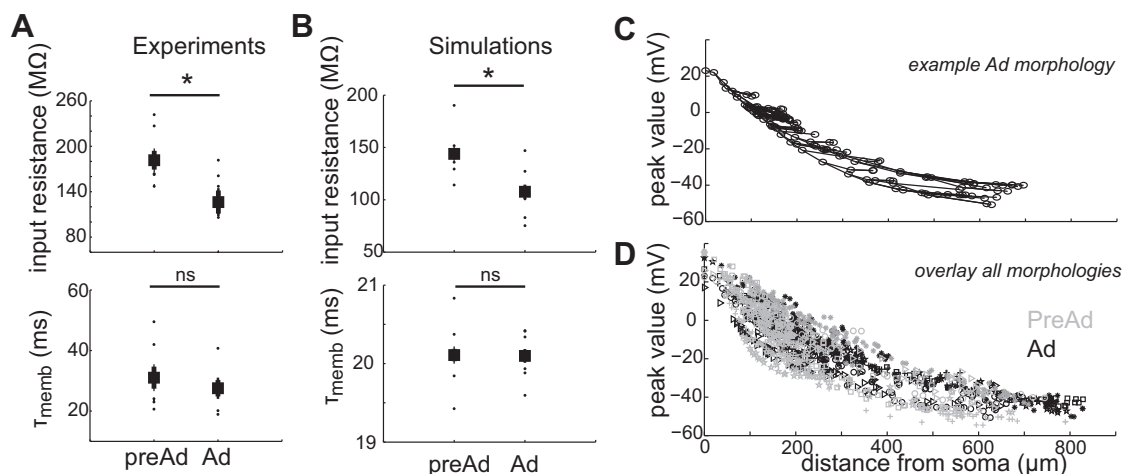


Fig. 3. Morphological development alone affects passive properties but does not alter backpropagation. *A*: passive membrane properties from experimental recordings in PreAd and Ad CA1 pyramidal neurons. *B*: passive membrane properties extracted from morphology reconstruction-based models ( $n = 6$  PreAd,  $n = 6$  Ad) in NEURON. *C*: distribution of BAP peak voltages across the dendritic tree in a model of an Ad neuron. Circles indicate dendritic regions measured. Lines indicate connected dendrites. *D*: overlay of both PreAd (gray symbols) and Ad (black symbols) neuron simulations showing similar distance-dependent BAP distributions. Symbols indicate individual neuron models.  $\tau_{\text{memb}}$ , Membrane time constant; ns, nonsignificant.  $*P < 0.05$ .

To directly determine whether the GABAergic regulation of plasticity was underpinned by changes in dendritic excitability, we measured AP backpropagation along apical dendrites and blocked all GABA(A) receptor-mediated inhibition (gabazine,  $10 \mu\text{M}$ ). In PreAd CA1 pyramidal neurons, there was no change in backpropagation of APs for either BAP(burst) or BAP(ss) into apical dendrites when GABA(A) receptors were blocked (Fig. 5A). The amplitude of the BAP-induced calcium transients with GABA(A) receptor blockers decreased linearly with distance, similar to the distance dependency observed in control conditions (aCSF) [Fig. 5A, linear regression slope BAP(ss): control ( $n = 6$  cells)  $-1.6 \pm 0.3$  (SD)  $\% \Delta F/R \cdot \text{mm}^{-1}$ , gabazine ( $10 \mu\text{M}$ ,  $n = 5$  cells)  $-1.6 \pm 0.3$  (SD)  $\% \Delta F/R \cdot \text{mm}^{-1}$ ; BAP(burst): control ( $n = 6$  cells)  $-3.9 \pm 0.5$  (SD)  $\% \Delta F/R \cdot \text{mm}^{-1}$ , gabazine ( $10 \mu\text{M}$ ,  $n = 5$  cells)  $-2.9 \pm 0.6$  (SD)  $\% \Delta F/R \cdot \text{mm}^{-1}$ ; two-way ANOVA BAP(ss)  $P = 0.54$ , BAP(burst)  $P = 0.41$ ].

In contrast, blockade of all GABA(A) receptor activity significantly modulated backpropagation along dendrites of Ad neurons. Backpropagation of AP bursts (Fig. 5B) was significantly enhanced in distal dendritic regions relative to control (250–450  $\mu\text{m}$  from soma,  $P < 0.001$ , two-way ANOVA followed by Bonferroni post hoc tests). BAP(ss) showed the same trend [distance 50% amplitude BAP(burst): control  $262 \pm 65 \mu\text{m}$  ( $n = 10$ ), gabazine ( $10 \mu\text{M}$ )  $493 \pm 81 \mu\text{m}$  ( $n = 6$ ),  $P < 0.001$ ; BAP(ss): control  $229 \pm 27 \mu\text{m}$  ( $n = 9$ ), gabazine ( $10 \mu\text{M}$ )  $292 \pm 54 \mu\text{m}$  ( $n = 2$ ),  $P = 0.35$ ]. Intriguingly, propagation into the proximal dendritic regions was not affected by blocking GABAergic inhibition, indicating a distance-dependent increase in dendritic inhibition. The kinetics, both rise and decay, of BAP-induced calcium transients were not distance dependent in either age group [Fig. 5, C and D, regression analysis (ANOVA) decay PreAd  $P = 0.54$ , Ad  $P = 0.57$ ; rise PreAd  $P = 0.76$ , Ad  $P = 0.088$ ]. However, the decay of fluorescent signals was significantly slower in PreAd compared with Ad dendrites [Fig. 5E, PreAd  $0.74 \pm 0.15$  s ( $n = 9$ ), Ad  $0.45 \pm 0.05$  s ( $n = 17$ ),  $P = 0.029$ ]. Furthermore, blockade of GABA(A) receptors resulted in a significantly slower decay of calcium transients in Ad dendrites, to a level not significantly

different from transients in PreAd dendrites [Fig. 5E, Ad control  $0.45 \pm 0.05$  s ( $n = 17$ ), Ad gabazine  $0.78 \pm 0.18$  s ( $n = 8$ ),  $P = 0.028$ ]. This modulation of calcium fluorescence decay kinetics by GABA(A) inhibition was not seen in younger dendrites [Fig. 5E, PreAd control  $0.74 \pm 0.15$  s ( $n = 9$ ), PreAd gabazine  $0.69 \pm 0.10$  s ( $n = 9$ ),  $P = 0.76$ ]. Thus upregulation in GABAergic inhibition onto CA1 pyramidal neuron dendrites during late postnatal development significantly attenuated backpropagation in more distal but not proximal regions of Ad dendrites only.

GABAergic inhibition manifests itself in two ways: fast phasic (milliseconds) and slow tonic (seconds) inhibition, mediated by different receptor subunits and involved in different dendritic functions (Brickley and Mody 2012). In the hippocampus, tonic GABAergic currents are mediated by the  $\delta$  and  $\alpha 5$  GABA(A) receptor subunits (Caraiscos et al. 2004; Scimemi et al. 2005). In addition, we have shown that STDP induction rules are dependent on tonic GABAergic inhibition (Fig. 4). We therefore investigated which subunit was responsible for the GABAergic modulation of BAP in Ad neurons. Specific blockade of  $\alpha 5$ -mediated tonic GABA(A) currents with the antagonist L-655,708 (100 nM) had no effect on spontaneous phasic GABAergic inhibition (data not shown). However, it caused strong modulation of BAP-induced calcium transients in distal dendrites, similar to effects of gabazine at  $10 \mu\text{M}$  [Fig. 6, A and B, distance 50% amplitude control  $262 \pm 65 \mu\text{m}$  ( $n = 10$ ), L-655,708  $417 \pm 14 \mu\text{m}$  ( $n = 6$ ), gabazine ( $10 \mu\text{M}$ )  $493 \pm 81 \mu\text{m}$  ( $n = 5$ ),  $P < 0.001$  compared with aCSF control conditions]. This modulation by  $\alpha 5$ -mediated GABA(A) receptors was seen for both BAP(ss) and BAP(burst) [distance 50% amplitude BAP(ss) control  $229 \pm 27 \mu\text{m}$  ( $n = 9$ ), L-655,708  $336 \pm 21 \mu\text{m}$  ( $n = 4$ ),  $P = 0.034$ , BAP(burst) control  $262 \pm 65 \mu\text{m}$  ( $n = 10$ ), L-655,708  $417 \pm 14 \mu\text{m}$  ( $n = 6$ ),  $P < 0.001$ ].

Tonic GABA(A) currents mediated by the  $\delta$ -subunit were specifically enhanced using THIP ( $10 \mu\text{M}$ ) (Olmos-Serrano et al. 2010). THIP had no effect on amplitudes of the calcium transients [Fig. 6, A and B, distance 50% amplitude control  $262 \pm 65 \mu\text{m}$  ( $n = 10$ ), THIP  $264 \pm 77 \mu\text{m}$  ( $n = 10$ ),  $P = 0.95$ ],



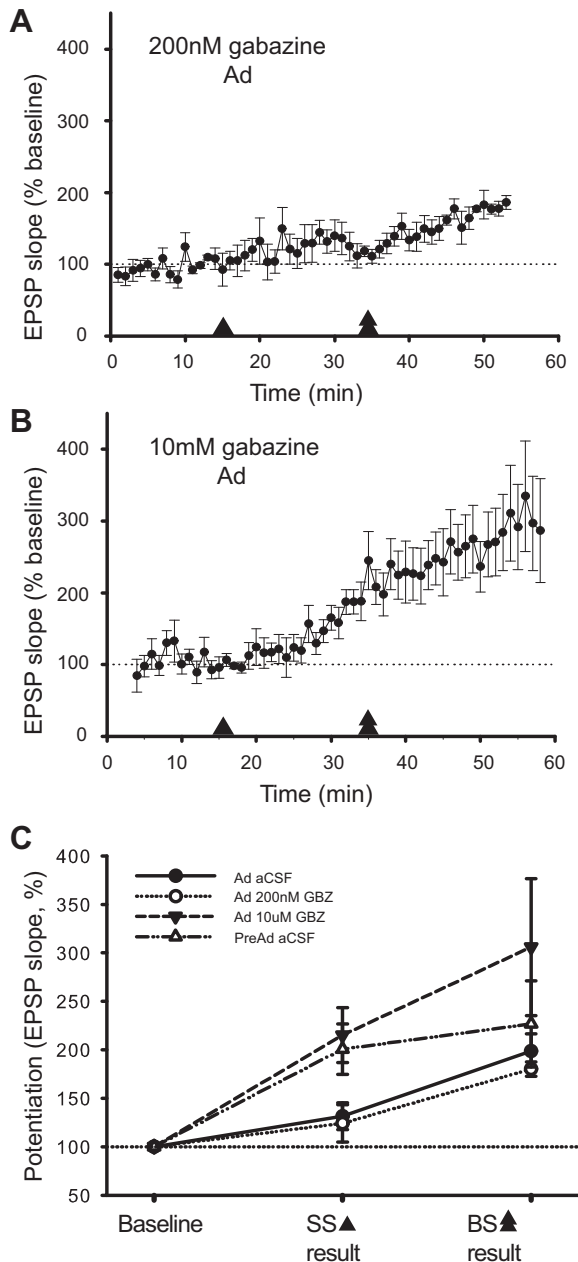


Fig. 4. Tonic inhibition regulates threshold for tLTP in Ad neurons. **A:** monitoring of EPSP slope following single-spike (SS) and subsequent burst (BS) pairing from baseline for Ad neurons in 200 nM gabazine (GBZ). Arrowhead indicates period of SS pairing, and double arrowheads indicate BS pairing period. Change in EPSP slope is expressed as a percent change relative to the last 3 min of baseline. **B:** change in EPSP slope following SS and BS pairing in Ad neurons in 10  $\mu$ M GBZ. **C:** summary graph of induced plasticity (%increase in EPSP slope) for PreAd and Ad neurons in the presence of control aCSF, blocking phasic and tonic GABA(A) receptors in Ad neurons (10  $\mu$ M GBZ) or blocking phasic GABA(A) receptors only in Ad neurons (200 nM GBZ). EPSP amplitudes after tLTP induction reflected the same dependence on tonic but not phasic GABA(A) receptor modulation as EPSP slope (data not shown).

indicating that  $\delta$ -subunits did not underlie the distance-dependent modulation of BAP. However, it significantly reduced the decay of the BAP-induced calcium transient [Fig. 6C,  $\tau$  decay control  $0.45 \pm 0.05$  s ( $n = 17$ ), THIP  $0.30 \pm 0.03$  s ( $n = 11$ ),  $P = 0.044$ ], suggesting a role for the GABA(A)  $\delta$ -subunit in BAP kinetics, but not BAP amplitude or spread. Therefore, the

developmental increase of GABA(A) receptor-mediated inhibition onto the distal dendrites of CA1 pyramidal neurons is mainly conferred by tonic  $\alpha 5$ -subunit-containing GABA(A) receptors that significantly attenuate dendritic excitability.

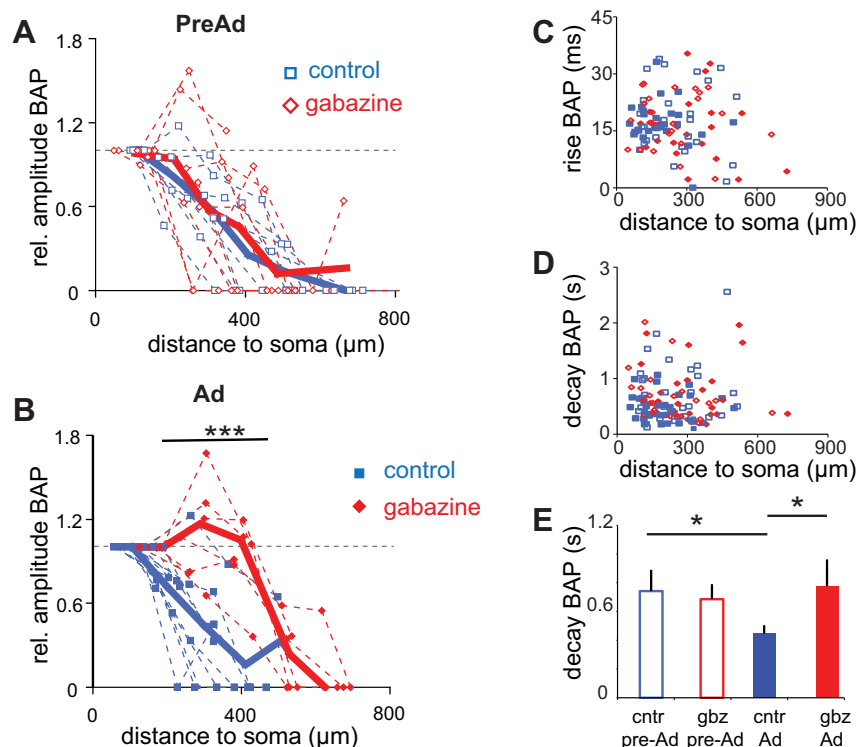
To directly show that  $\alpha 5$ -containing GABA(A) receptors mediate tonic currents in the distal dendrites, we measured local dendritic holding currents with dendritic patch-clamp recordings following blockade of GABA(A)  $\alpha 5$ -subunits (Fig. 7, A and B). Application of L-655,708 significantly altered tonic dendritic currents ( $8.9 \pm 2.2$  pA relative to baseline, aCSF:  $-27.6 \pm 6.5$  pA, L-655,708:  $-18.7 \pm 6.3$  pA,  $P = 0.016$  paired  $t$ -test,  $n = 5$ , Fig. 7, B and C). Subsequent infusion of 10  $\mu$ M of gabazine to block all GABA(A) receptors did not further change the holding current ( $9.4 \pm 4.0$  pA relative to  $8.9 \pm 2.2$  pA,  $P = 0.91$ ,  $n = 4$ , Fig. 7, B and C), demonstrating that Ad CA1 pyramidal dendrites showed prominent dendritic tonic currents which are mediated by  $\alpha 5$ -containing GABA(A) receptors.

Calcium transients in the dendrite, as measured by two-photon calcium imaging, result from activation of voltage-dependent calcium channels (Ross 2012). To test if  $\alpha 5$ -subunit-mediated effects were due to changes in AP backpropagation of voltage or due to GABAergic effects upon calcium stores or channels, we made dendritic patch-clamp recordings in regions where the most prominent inhibitory modulation was observed (Fig. 5). We measured dendritic AP amplitudes, induced by a depolarizing step, before and after the application of the  $\alpha 5$ -subunit-specific antagonist, L-655,708 (Fig. 8A). Peak dendritic voltage showed a significant increase after blocking  $\alpha 5$  GABA(A) receptor subunits [Fig. 8B, BAP amplitude from baseline membrane potential ( $V_m$ ), pre  $71.6 \pm 2.5$ , post  $74.0 \pm 2.6$  mV ( $n = 10$ ),  $P = 0.039$ ], in line with increased dendritic transients recorded in the calcium imaging experiments. No significant increase was observed in aCSF controls (Fig. 8C,  $P = 0.36$ ). In contrast to dendrites, no significant change in BAP amplitude was observed at the soma following blockade of  $\alpha 5$ -specific inhibition (Table 1). These data suggest that, similar to GABAergic regulation of dendritic calcium transients, the voltage signal of the BAP is also modulated by  $\alpha 5$ -subunit-mediated tonic inhibition in a dendrite-specific manner.

To further investigate the spatial extent of tonic GABAergic modulation both at the soma and in the dendrites, we tested the effects of GABA-receptor modulating drugs on somatic function. Both in PreAd and Ad neurons, there was no effect of  $\alpha 5$ -receptor subunit blockade on passive ( $V_m$ , membrane  $\tau$ , input resistance), or active properties (AP peak, AP halfwidth, AP threshold) measured at the soma (Table 1). These somatic recordings do not reliably detect distal dendritic tonic currents due to strong attenuation within the dendrites and limited spatial reach of somatic voltage clamp (Williams and Mitchell 2008). Together with the observation that proximal dendrites were not affected by blocking GABA(A)-mediated inhibition (Figs. 5C and 6A) and distal dendrites show prominent  $\alpha 5$ -GABA(A) subunit-mediated tonic current (Fig. 7), this indicates that the prominent effect of  $\alpha 5$ -subunit-mediated tonic inhibition is specifically targeted toward distal dendritic regions.

Both interneurons and astrocytes, the potential sources of tonic inhibition, target specific regions of the dendrites (Heja et al. 2012; Klausberger 2009), creating different spatial cover-

Fig. 5. GABAergic inhibition regulates BAP in distal dendrites of Ad neurons. *A*: similar distance-dependent BAP profiles along apical dendrite in control aCSF or GBZ (10  $\mu$ M) in PreAd neurons. Multiple distances from the soma were recorded for each cell. Distance-dependent amplitudes of calcium transients are shown normalized to the first proximal dendritic recording at 100  $\mu$ m within each dendrite. Dashed lines indicate individual recordings; solid line shows the binned average per 100  $\mu$ m. *B*: significant alteration in distance-dependent BAP along apical dendrite in control conditions or GBZ (10  $\mu$ M) in Ad neurons. Solid lines show the average; dashed lines indicate individual cell recordings. *C* and *D*: distribution of rise and decay times according to age group and control/GBZ recording conditions. Key symbols are indicated in *B*. *E*: significant alteration in decay time constant of fluorescence signal in Ad neurons in presence of GBZ. Data for amplitude and kinetics of the calcium transients and effects of GBZ after BAP(burst) are shown. Single-spike BAP [BAP(ss)] shows similar modulation by GABA(A) receptor blockade (values given in text). \* $P < 0.05$ . \*\*\* $P < 0.001$ .



age. In addition, ion channels, such as HCN channels, show a spatially regulated distribution along CA1 pyramidal dendrites (Hoffman et al. 1997; Magee 1998; Nestor and Hoffman 2012b). To test which spatial distribution of tonic GABA inhibition in dendrites could explain our observations, we implemented a well-established active model of a mature CA1 pyramidal neuron on to a reconstructed Ad neuron (Poirazi et al. 2003; Sterratt et al. 2012). Tonic GABA(A) conductances (Pavlov et al. 2009) were inserted in the apical dendrite with differing spatial gradients of expression: distributed uniformly along the somato-dendritic axis, in a distally increasing gradient, in a distally decreasing gradient or restricted to a localized distal dendritic region (Fig. 9, A–C). Distally decreasing gradients and uniform expression profiles resulted in a reduced AP height at the soma (Fig. 9D). In addition, these distribution patterns had their most prominent effect on calcium currents in more proximal regions of the dendrites (Fig. 9E). In contrast, localized dendritic expression and distally increasing dendritic profiles had little effect on the soma (Fig. 9D), but produced strong reduction of the calcium signal in the distal dendrites, supporting our experimental findings (Figs. 9E and 5). These results demonstrate that attenuation of dendritic BAP can result from a distally increasing expression gradient or a localized distal region of tonic GABA(A) receptor expression in the dendrites of Ad CA1 pyramidal neurons.

## DISCUSSION

Dendritic excitability plays a crucial role in regulating information processing and memory storage in the hippocampus (Lee et al. 2012; Sjostrom et al. 2008). Our data show that tonic GABAergic inhibition mediated via  $\alpha 5$ -containing GABA(A) receptors is a strong regulator of distal dendritic excitability and synaptic plasticity in CA1 pyramidal neurons. This is developmentally regulated: only dendrites from Ad brains

exhibit this tonic GABAergic modulation. Model simulations demonstrate that these findings are consistent with a distally increasing or a localized distal expression of dendritic tonic inhibition.

We show that effects of tonic GABA(A)  $\alpha 5$ -receptor-mediated inhibition on excitability are exerted in distal dendrites but not at the soma of Ad neurons.  $\alpha 5$ -Receptor-mediated currents regulate tonic inhibition locally and attenuate the amplitude of somatically generated BAPs. From model simulations, we find that the attenuation of dendritic BAP can be accounted for by distance-dependent tonic inhibition, similar to increasing distance gradients reported for voltage-gated ion channels, h channels and A-type potassium channels (Hoffman et al. 1997; Magee et al. 1998; Nestor and Hoffman 2012a). Our model findings of dendrite-specific localization of tonic currents are consistent with immunohistology:  $\alpha 5$ -containing GABA receptors are predominantly expressed in the dendritic layers of CA1 hippocampus during this Ad period of development (Hutcheon et al. 2004; Ramos et al. 2004). In the distal SR, the majority of GABAergic inputs to CA1 pyramidal neurons are made on to dendritic shafts (Megias et al. 2001), the same region where we also observed the strongest modulation of calcium transients by BAP. These GABAergic inputs made directly on dendrites are proposed to mediate tonic inhibitory currents (Brickley and Mody 2012). Here, we now show at a functional level that  $\alpha 5$ -mediated tonic receptors on distal dendrites effectively regulate dendritic excitability.

During pyramidal cell development, the total length of apical and basal dendrites increases, while at the same time firing pattern shifts from regular to burst firing (Degenetais et al. 2002; Franceschetti et al. 1998; Zhang 2004). This change in firing pattern may be directly attributable to increased dendritic size (van Elburg and van Ooyen 2010). However, as we have shown here, these developmental changes in morphol-



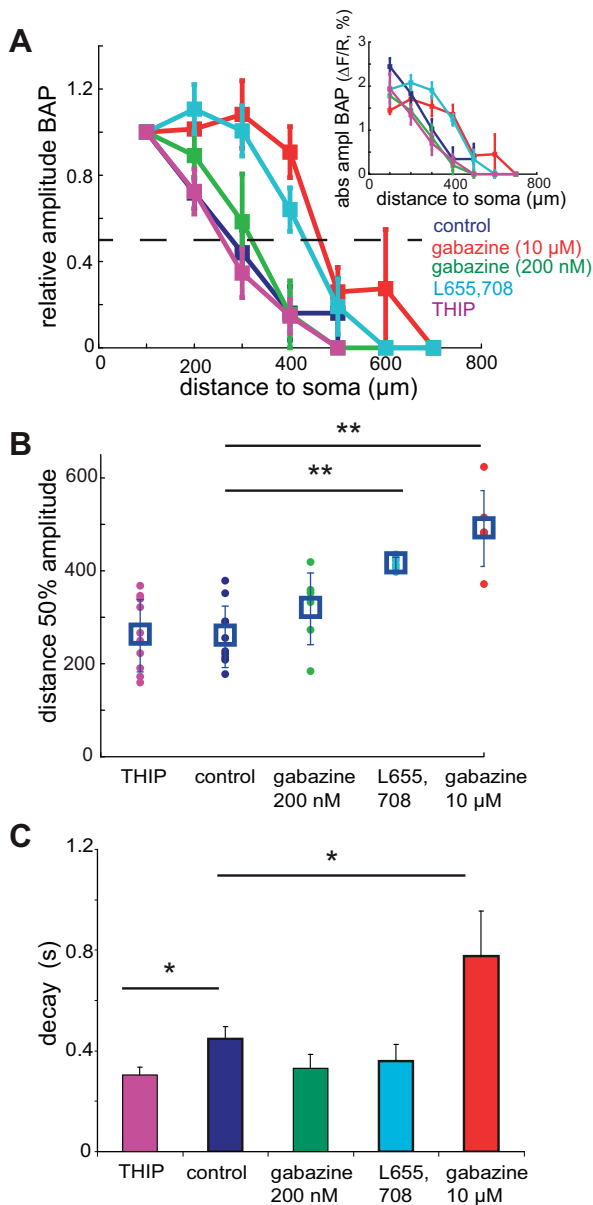


Fig. 6.  $\alpha 5$ -Mediated tonic GABA(A) receptors are responsible for the BAP modulation in Ad neurons. **A**: distance-dependent BAP(burst) in Ad (P28–46) neurons in control conditions (dark blue), 200 nM GBZ (green), 10  $\mu\text{M}$  GBZ (red), L-655,708 (light blue) and THIP (purple). Multiple distances from the soma were recorded for each cell. Amplitudes are shown relative to the first proximal dendritic recording at 100  $\mu\text{m}$ . Dashed line indicates 50% relative amplitude. Binned averages are shown. *Inset*: absolute amplitudes ( $\Delta F/R$ ) plotted against distance from soma for all conditions. **B**: quantification of the BAP modulation by GABA(A) receptor subunit-mediated inhibition using the distance at which the calcium transient amplitude was 50% of the first proximal recording. Significant differences in distance of 50% amplitude occur between L-655,708 and GBZ (10  $\mu\text{M}$ ) conditions compared with control. Individual values and mean  $\pm$  SE distribution are shown. **C**: significant alteration in decay time constant of dendritic fluorescence signal in presence of THIP or GBZ (10  $\mu\text{M}$ ) compared with control. \* $P < 0.05$ . \*\* $P < 0.01$ .

ogy cannot explain the difference in AP backpropagation between Ad and the more immature, PreAd neurons.

Modulation of dendritic excitability by ligand-gated GABAergic ion channels complements the modulation of dendritic APs via voltage-gated ion channels, including A-type potassium and  $I_h$  channels (Andrasfalvy et al. 2008; Magee et

al. 1998). The expression levels of some of these channels also alter during Ad maturation (Bender et al. 2001; Guan et al. 2011; Maletic-Savatic et al. 1995; Vasilyev and Barish 2002). Intriguingly, the L-type voltage-gated calcium channel, Cav 1.3, only reaches mature levels in the second postnatal month in rodents (Glazewski et al. 1993; Kramer et al. 2012). It is tempting to speculate that this developmental increase in excitability by calcium channels might counteract the increased inhibition mediated via  $\alpha 5$ -containing GABA receptors. In our study, we were able to show that the increased inhibition via  $\alpha 5$ -containing GABA receptors in Ad neurons could explain the altered synaptic plasticity thresholds during development. Levels of excitation and inhibition are kept in a regulatory balance during development and adulthood, a phenomenon called homeostatic scaling (Liu 2004; Mody 2005). Tonic inhibition plays an important role in maintaining the excitation/inhibition balance, as evidenced by the strong upregulation of tonic GABA(A) receptor-mediated currents following the knock-out of excitatory h- or A-type potassium currents (Andrasfalvy et al. 2008; Chen et al. 2010). Development of excitation/inhibition balance as well as the dendritic expression levels of these channels need to be subject to further investigation.

A dendrite-specific localization of tonic inhibition is in line with recent proposals that dendritic compartments act as independent functional units within a neuron where different regions have different functions (Branco et al. 2010). Both excitatory and inhibitory projections onto pyramidal cells are targeted to specific dendritic compartments, depending on presynaptic cell type and brain region, in this way creating different functional regions within the cell (Klausberger 2009; Royer et al. 2012; van Strien et al. 2009). In the hippocampus in vivo, dendritically targeted inhibition changes both frequency and firing mode of pyramidal neurons, depending on their place field selectivity (Royer et al. 2012). In contrast, in the same study somatic inhibition was found to affect only the phase of spiking. Here, we show that tonic currents are specifically directed onto dendritic compartments, controlling both excitability and plasticity in distal dendrites, without affecting somatic function. Given this restricted dendritic compartmentalization, we hypothesize that activating tonic inhibition will enhance the effect of perisomatic inputs upon the soma relative to distal inputs by reducing dendritic excitability.

Tonic inhibitory currents have significant implications for dendritic computation (Fernandez and White 2010; Pavlov et al. 2009). Due to the larger dendritic membrane area covered by tonic extrasynaptic contacts compared with phasic synaptic contacts, activation of tonic receptors causes a larger charge transfer than activation of synaptic receptors alone (Brunig et al. 2002; Olsen and Sieghart 2009). Therefore, tonic receptors, located on dendritic shafts, are optimal candidates to directly modulate dendritic excitability and thereby dendritic computation (Fernandez and White 2010; Pavlov et al. 2009). Our data show that GABA(A) receptor-mediated tonic neurotransmission modulated dendritic excitability (Figs. 5 and 6). This effect occurs locally in dendrites, is developmentally regulated and only observed in Ad neurons. One direct functional consequence of increased tonic GABAergic inhibition is that Ad neurons require a burst of APs rather than SSs for synaptic plasticity (Fig. 1). Tonic GABA(A)-mediated inhibition regulated the threshold for induction of tLTP, in agreement with a

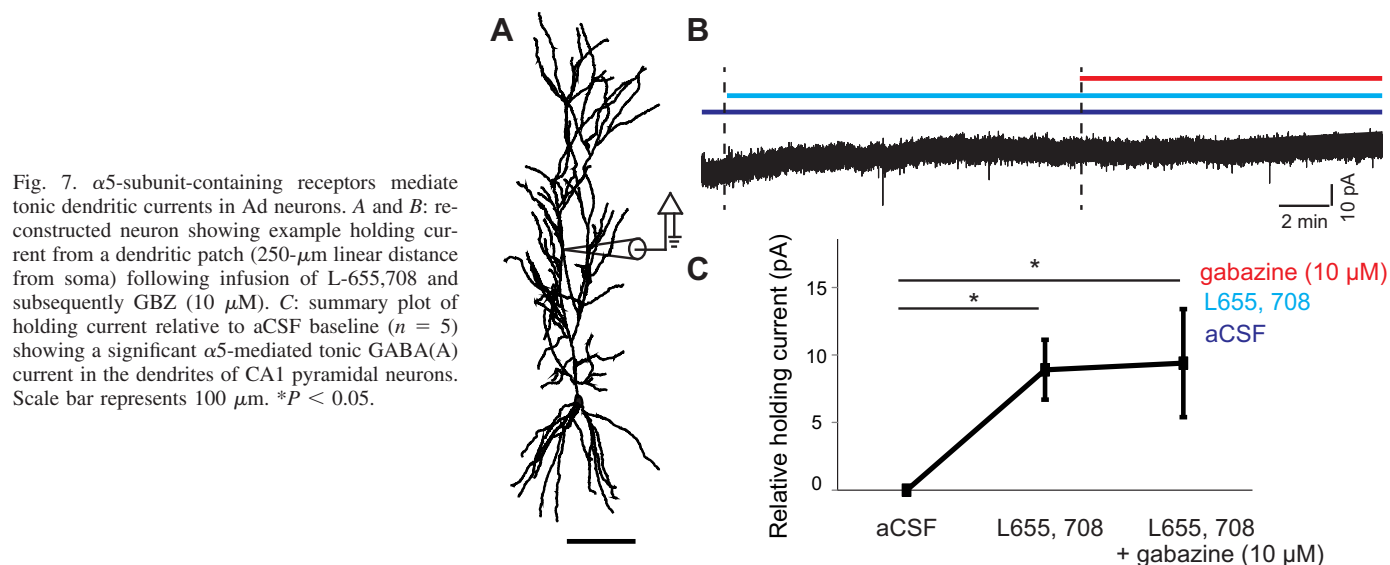


Fig. 7.  $\alpha 5$ -subunit-containing receptors mediate tonic dendritic currents in Ad neurons. *A* and *B*: re-constructed neuron showing example holding current from a dendritic patch (250- $\mu$ m linear distance from soma) following infusion of L-655,708 and subsequently GBZ (10  $\mu$ M). *C*: summary plot of holding current relative to aCSF baseline ( $n = 5$ ) showing a significant  $\alpha 5$ -mediated tonic GABA(A) current in the dendrites of CA1 pyramidal neurons. Scale bar represents 100  $\mu$ m. \* $P < 0.05$ .

decreased threshold for theta-frequency LTP induction in  $\alpha 5$  GABA(A) knockout mice (Martin et al. 2010).

In this study, we have focused on the role of dendritic excitability modulation during development. We have shown that GABAergic modulation could explain a difference in plasticity induction requirements. However, this does not exclude additional developmental changes occurring simultaneously at the site of origin, the synapse. Changes in calcium influx at the spine via postsynaptic voltage-gated calcium channel expression (Jones et al. 1997) or developmental regulation of synaptic protein kinases underlying hippocampal plasticity (Luchkina et al. 2014; Yasuda et al. 2003) could also

contribute to changes in induction thresholds during postnatal maturation.

In the hippocampus, tonic inhibitory currents are mediated by the  $\alpha 5$  and  $\delta$  GABA(A) receptor subunits (Brickley and Mody 2012), which are both located at peri- and extrasynaptic sites. In our study, blocking of both phasic and tonic inhibition resulted in the same modulation of BAP as blocking tonic inhibition alone (Figs. 5 and 6). The distance-dependent modulation of BAP was fully accounted for by  $\alpha 5$ -mediated tonic currents (Fig. 6). Intriguingly, dendritic  $\alpha 5$ -mediated regulation was observed for both calcium transients and voltage deflections, suggesting a direct action on voltage propagation. In addition to regulation by the  $\alpha 5$ -subunit, we found a small change in calcium fluorescence kinetics in Ad dendrites, in agreement with dendrite-specific  $\delta$ -subunit expression in the mature hippocampus (Sperk et al. 1997), but this did not affect the range of BAP, which was solely regulated by  $\alpha 5$ -subunit mediated GABAergic inhibition. During puberty, an upregulation in  $\alpha 4\beta\delta$ -containing GABA(A) receptors occurs in CA1 hippocampus of female mice, which also impairs LTP induction and, furthermore, impairs spatial learning (Shen et al. 2010). However, in agreement with our findings in CA1 pyramidal neurons from Ad mice, the majority of tonic inhibition measured at the soma in young adult rodents is mediated by  $\alpha 5$ , with only a small residual component mediated either via the  $\delta$ -subunit or receptors containing only  $\alpha$ - or  $\beta$ -subunits (Glykys et al. 2008). The specific role of the  $\delta$ -subunit in the kinetics of the BAP requires further investigation and would benefit from the development of a specific antagonist in addition to the currently available agonist THIP.

In rodents, GABAergic function in the hippocampus continues to mature beyond weaning up to the second postnatal month (Banks et al. 2002; Cohen et al. 2000; Danglot et al. 2006). We verified this protracted development of GABAergic inhibition at the electron-microscopic level by the significant development of the synapse and synaptic vesicles at symmetric synapses during late postnatal development (Fig. 1). Consequently, we found a developmental increase in dendritic tonic GABA(A) receptor-mediated modulation of BAP (Figs. 5 and 6). This enhancement of tonic inhibition is consistent with a

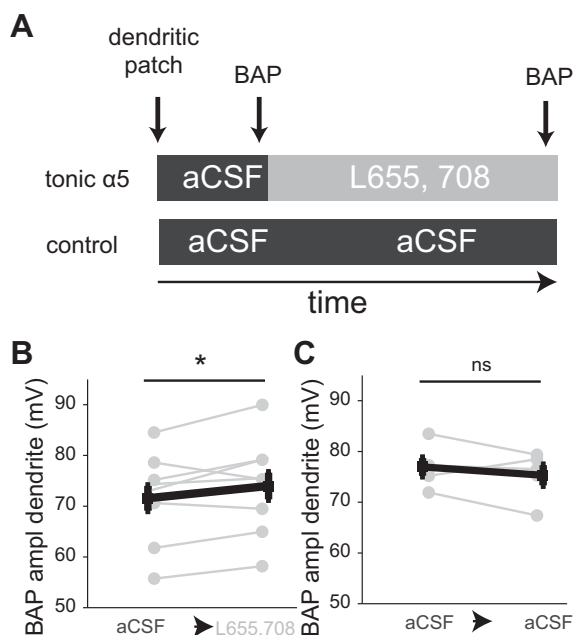


Fig. 8.  $\alpha 5$ -Mediated tonic currents in dendrites modulate BAP in Ad neurons. *A*: experimental paradigm. BAP was induced by a depolarizing step in the dendrite, and both peak and input resistance were assessed in the presence of aCSF (control conditions). L-655,708 or aCSF was bath applied for 20 min, after which BAP was again measured in the dendrites. *B*: BAP amplitude before and after application of L-655,708. *C*: BAP amplitude before and after bath application of aCSF (control). \* $P < 0.05$ .

Table 1. Active and passive properties of young (postnatal days 14–19) and mature (postnatal days 28–46) CA1 pyramidal neurons based on spike profile before and after the application of the GABA(A) targeted drugs gabazine (10  $\mu$ M and 200 nM), THIP, and L-655,708, or artificial cerebrospinal fluid

	<i>n</i>	<i>V<sub>m</sub></i> , mV		<i>R<sub>m</sub></i> , MΩ		<i>τ</i> , ms		AP Threshold, mV		AP Halfwidth, ms		AP Peak, mV	
		Pre	Post	Pre	Post	Pre	Post	Pre	Post	Pre	Post	Pre	Post
Young CA1 pyramidal neurons													
Control	8	-64.1 ± 1.5	-58.1 ± 1.1	181.6 ± 12.4	179.5 ± 23.5	31.0 ± 3.6	39.2 ± 6.8	-41.8 ± 0.5	-40.8 ± 0.4	1.32 ± 0.07	1.23 ± 0.06	71.6 ± 2.9	73.1 ± 3.1
Gabazine (10 μM)	17	-65.9 ± 0.8	-59.6 ± 1.1	160.8 ± 11.6	157.7 ± 14.1	30.8 ± 2.6	35.1 ± 4.2	-43.9 ± 1.0	-42.0 ± 1.4	1.44 ± 0.09	1.33 ± 0.08	73.3 ± 1.9	72.3 ± 2.2
Pre-post		**		ns		**		ns		*		ns	
Drug pre-post*		ns		ns		ns		ns		ns		ns	
Mature CA1 pyramidal neurons													
Control	7	-65.6 ± 1.2	-60.6 ± 1.5	126.3 ± 15.3	100.6 ± 10.0	27.5 ± 2.7	24.3 ± 2.1	-43.6 ± 2.2	-41.8 ± 1.6	1.32 ± 0.12	1.12 ± 0.08	90.1 ± 3.2	85.5 ± 2.9
Gabazine (10 μM)	14	-64.6 ± 0.8	-58.9 ± 1.5	110.9 ± 8.8	91.6 ± 7.8	31.7 ± 4.2	27.4 ± 2.3	-41.1 ± 1.0	-38.3 ± 1.6	1.20 ± 0.06	1.08 ± 0.04	78.5 ± 2.1	77.1 ± 1.6
Gabazine (200 nM)	5	-69.3 ± 1.4	-60.9 ± 0.7	103.8 ± 8.2	94.5 ± 7.4	20.6 ± 1.5	20.2 ± 2.9	-47.6 ± 1.1	-40.4 ± 2.3	1.14 ± 0.04	1.03 ± 0.04	75.5 ± 1.8	77.1 ± 3.0
THIP	7	-65.3 ± 0.8	-60.6 ± 1.5	125.6 ± 16.0	88.2 ± 8.4	24.3 ± 2.7	17.3 ± 1.4	-42.0 ± 1.5	-39.7 ± 2.0	1.27 ± 0.05	1.28 ± 0.08	89.4 ± 2.4	81.5 ± 4.6
L-655,708	7	-64.8 ± 1.6	-60.5 ± 0.9	148.4 ± 34.4	106.1 ± 6.5	18.7 ± 1.1	13.6 ± 2.4	-48.5 ± 0.8	-44.7 ± 1.1	1.25 ± 0.06	1.13 ± 0.04	81.3 ± 2.5	76.9 ± 3.6
Pre-post		**		**		ns		**		**		**	
Drug pre-post*		ns		ns		ns		ns		ns		ns	

Values are means  $\pm$  SE; *n*, no. of neurons.  $V_m$ , membrane potential;  $R_m$ , input resistance;  $\tau$ , time constant; AP, action potential; Pre, before application; Post, after application. Tonic inhibition does not alter somatic passive and active properties. Active and passive properties of preadolescent (postnatal days 14–19) and adolescent (postnatal days 28–46) CA1 pyramidal neurons based on spike profile before (pre) and after (post) the application of the GABA(A) targeted drugs [gabazine (10  $\mu$ M and 200 nM), THIP, and L-655,708] or artificial cerebrospinal fluid are shown. Statistical analysis is based on repeated-measures mixed ANOVA. Significant difference: \* $P$  < 0.05, \*\* $P$  < 0.01, or not significant (ns).

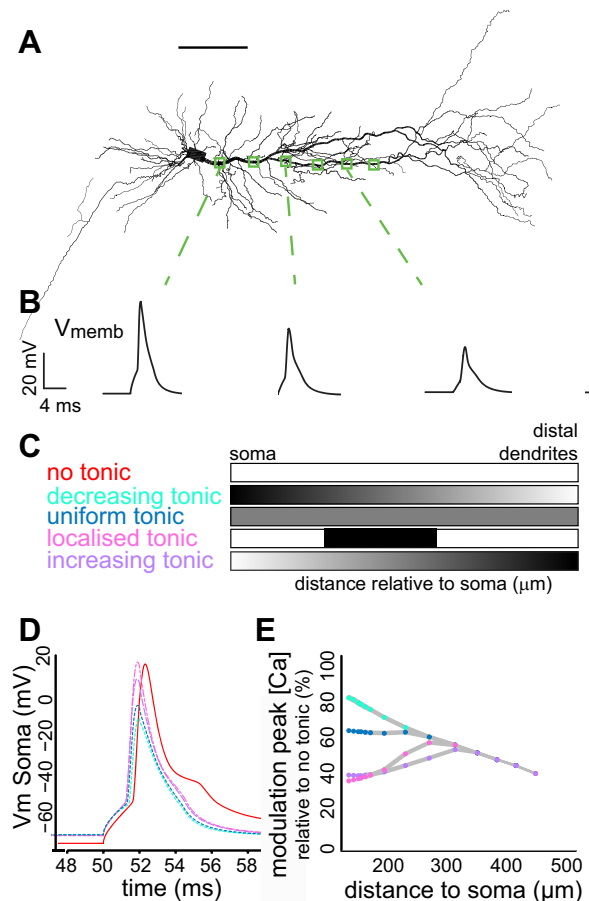


Fig. 9. Model predicts localized or increasing tonic GABA(A) receptor distribution. **A**: morphology of a reconstructed Ad neuron incorporated in a NEURON model containing a realistic set of active and passive properties of adult CA1 pyramidal neurons based on (Sterratt et al. 2012). Scale bar represents 100  $\mu$ m. **B**: example traces of voltage deflections at the locations indicated in **A**, in the presence of uniform tonic currents. **C**: tonic GABA(A) conductance, as measured by Pavlov et al. (2009), was distributed in the apical dendrite of the model according to different spatial distributions: distally increasing, distally decreasing, uniform or no tonic inhibition at all. In addition, a localized expression of tonic GABA(A) in the apical dendrite between 200 and 400  $\mu$ m from the soma was also simulated. **D**: effect of the different tonic GABA(A) distributions on somatic action potential shape. Colors correspond to **C**. Distally decreasing and uniform distributions show strong effects on somatic properties, while distally increasing and localized distributions have little impact on somatic AP properties. **E**: modulation of dendritic calcium currents by the different dendritic tonic GABA(A) distributions relative to no tonic currents plotted against distance to soma. Colors correspond to **C**. Localized and distally increasing distributions have their main effect in distal dendrites.  $V_{memb}$  and  $V_m$ , membrane potential.

dendritic expression of tonic GABA(A) subunits in SR and SLM during postnatal development (Ramos et al. 2004; Shen et al. 2010). These developmental changes in dendritic excitability markedly affect the cell's computational properties and plasticity characteristics (Figs. 1 and 4), underlining the importance of using older pyramidal neurons in electrophysiological studies that purport to examine information processing in adulthood.

The source of tonic inhibition is currently not well defined. CA1 pyramidal neurons receive inhibition from many different types of interneurons, all projecting to specific parts of the soma, axon or the dendritic tree (Klausberger 2009). However, whether one interneuron type can activate both phasic and



tonic receptors, the latter via spillover (Glykys and Mody 2007), or whether interneurons specialize in one of the two types of inhibition is as yet unclear. In addition, astrocytes can also release GABA into the extracellular space (Brickley and Mody 2012; Farrant and Nusser 2005; Heja et al. 2012) and could thereby regulate dendritic excitability of the hippocampus. Our data show that effects of tonic GABA(A) receptor-mediated inhibition are not uniform along apical dendrites, suggesting localized GABA release from distal dendrite-targeting interneurons or astrocytes.

In summary, we have shown that dendritically targeted  $\alpha 5$ -mediated tonic inhibition regulates dendritic excitability and STDP in a developmental manner. Our mechanistic data show that dendrite and soma are differently regulated by tonic  $\alpha 5$ -mediated inhibition, which has important implications for dendritic computation and hippocampal function.

## ACKNOWLEDGMENTS

We thank Christiaan de Kock for biocytin staining.

Present address of E. Pérez-García: Department of Biomedicine, Institute of Physiology, Pharmazentrum, University of Basel, Basel, Switzerland.

## GRANTS

This work was supported by grants from the Nederlandse Organisatie voor Wetenschappelijk Onderzoek to R. M. Meredith (ZonMW no. 917.10.372) and M. R. Groen (TopTalent no. 021.002.082). M. R. Groen was also supported by a Network of European Neuroscience Schools training studentship. A. v. Ooyen was partly supported by the Self-Constructing Computing Systems project (216593) of the Seventh Framework Programme of the European Union.

## DISCLOSURES

No conflicts of interest, financial or otherwise, are declared by the author(s).

## AUTHOR CONTRIBUTIONS

Author contributions: M.R.G., O.P., E.P.-G., T.N., H.D.M., and R.M.M. conception and design of research; M.R.G., J.W., M.D., and R.M.M. performed experiments; M.R.G., J.W., M.D., and R.M.M. analyzed data; M.R.G., O.P., M.D., A.v.O., and R.M.M. interpreted results of experiments; M.R.G. and R.M.M. prepared figures; M.R.G., A.v.O., and R.M.M. drafted manuscript; M.R.G., A.v.O., and R.M.M. edited and revised manuscript; M.R.G., O.P., E.P.-G., T.N., J.W., M.D., H.D.M., A.v.O., and R.M.M. approved final version of manuscript.

## REFERENCES

- Abramoff MD, Magalhaes PJ, Ram SJ. Image processing with ImageJ. *Biophotonics International* 11: 36–42, 2004.
- Andrasfalvy BK, Makara JK, Johnston D, Magee JC. Altered synaptic and non-synaptic properties of CA1 pyramidal neurons in Kv4.2 knockout mice. *J Physiol* 586: 3881–3892, 2008.
- Banks MI, Hardie JB, Pearce RA. Development of GABA(A) receptor-mediated inhibitory postsynaptic currents in hippocampus. *J Neurophysiol* 88: 3097–3107, 2002.
- Belelli D, Harrison NL, Maguire J, Macdonald RL, Walker MC, Cope DW. Extrasynaptic GABAA receptors: form, pharmacology, and function. *J Neurosci* 29: 12757–12763, 2009.
- Bender RA, Brewster A, Santoro B, Ludwig A, Hofmann F, Biel M, Baram TZ. Differential and age-dependent expression of hyperpolarization-activated, cyclic nucleotide-gated cation channel isoforms 1–4 suggests evolving roles in the developing rat hippocampus. *Neuroscience* 106: 689–698, 2001.
- Branco T, Clark BA, Hausser M. Dendritic discrimination of temporal input sequences in cortical neurons. *Science* 329: 1671–1675, 2010.
- Brickley SG, Mody I. Extrasynaptic GABA(A) receptors: their function in the CNS and implications for disease. *Neuron* 73: 23–34, 2012.
- Brunig I, Scotti E, Sidler C, Fritschy JM. Intact sorting, targeting, and clustering of gamma-aminobutyric acid A receptor subtypes in hippocampal neurons in vitro. *J Comp Neurol* 443: 43–55, 2002.
- Buchanan KA, Mellor JR. The development of synaptic plasticity induction rules and the requirement for postsynaptic spikes in rat hippocampal CA1 pyramidal neurons. *J Physiol* 585: 429–445, 2007.
- Bureau I, von Saint Paul F, Svoboda K. Interdigitated paralemniscal and lemniscal pathways in the mouse barrel cortex. *PLoS Biol* 4: e382, 2006.
- Campanac E, Debanne D. Spike timing-dependent plasticity: a learning rule for dendritic integration in rat CA1 pyramidal neurons. *J Physiol* 586: 779–793, 2008.
- Caraiscos VB, Elliott EM, You-Ten KE, Cheng VY, Belelli D, Newell JG, Jackson MF, Lambert JJ, Rosahl TW, Wafford KA, MacDonald JF, Orser BA. Tonic inhibition in mouse hippocampal CA1 pyramidal neurons is mediated by alpha 5 subunit-containing gamma-aminobutyric acid type A receptors. *Proc Natl Acad Sci U S A* 101: 3662–3667, 2004.
- Chen X, Shu S, Schwartz LC, Sun C, Kapur J, Bayliss DA. Homeostatic regulation of synaptic excitability: tonic GABAA receptor currents replace Ih in cortical pyramidal neurons of HCN1 knock-out mice. *J Neurosci* 30: 2611–2622, 2010.
- Cohen AS, Lin DD, Coulter DA. Protracted postnatal development of inhibitory synaptic transmission in rat hippocampal area CA1 neurons. *J Neurophysiol* 84: 2465–2476, 2000.
- Danglot L, Triller A, Marty S. The development of hippocampal interneurons in rodents. *Hippocampus* 16: 1032–1060, 2006.
- Degenetais E, Thierry AM, Glowinski J, Gioanni Y. Electrophysiological properties of pyramidal neurons in the rat prefrontal cortex: an in vivo intracellular recording study. *Cereb Cortex* 12: 1–16, 2002.
- Dudek SM, Bear MF. Bidirectional long-term modification of synaptic effectiveness in the adult and immature hippocampus. *J Neurosci* 13: 2910–2918, 1993.
- Farrant M, Nusser Z. Variations on an inhibitory theme: phasic and tonic activation of GABA(A) receptors. *Nat Rev Neurosci* 6: 215–229, 2005.
- Feldman DE. The spike-timing dependence of plasticity. *Neuron* 75: 556–571, 2012.
- Fernandez FR, White JA. Gain control in CA1 pyramidal cells using changes in somatic conductance. *J Neurosci* 30: 230–241, 2010.
- Franceschetti S, Sancini G, Panzica F, Radici C, Avanzini G. Postnatal differentiation of firing properties and morphological characteristics in layer V pyramidal neurons of the sensorimotor cortex. *Neuroscience* 83: 1013–1024, 1998.
- Gasparini S, Losonczy A, Chen X, Johnston D, Magee JC. Associative pairing enhances action potential back-propagation in radial oblique branches of CA1 pyramidal neurons. *J Physiol* 580: 787–800, 2007.
- Glazewski S, Skangiel-Kramska J, Kossut M. Development of NMDA receptor-channel complex and L-type calcium channels in mouse hippocampus. *J Neurosci Res* 35: 199–206, 1993.
- Glykys J, Mann EO, Mody I. Which GABA(A) receptor subunits are necessary for tonic inhibition in the hippocampus? *J Neurosci* 28: 1421–1426, 2008.
- Glykys J, Mody I. The main source of ambient GABA responsible for tonic inhibition in the mouse hippocampus. *J Physiol* 582: 1163–1178, 2007.
- Golding NL, Kath WL, Spruston N. Dichotomy of action-potential back-propagation in CA1 pyramidal neuron dendrites. *J Neurophysiol* 86: 2998–3010, 2001.
- Guan D, Horton LR, Armstrong WE, Foehring RC. Postnatal development of A-type and Kv1- and Kv2-mediated potassium channel currents in neocortical pyramidal neurons. *J Neurophysiol* 105: 2976–2988, 2011.
- Heja L, Nyitrai G, Kekesi O, Dobolyi A, Szabo P, Fiath R, Ulbert I, Pal-Szenthe B, Palkovits M, Kardos J. Astrocytes convert network excitation to tonic inhibition of neurons. *BMC Biol* 10: 26, 2012.
- Hines ML, Carnevale NT. The NEURON simulation environment. *Neural Comput* 9: 1179–1209, 1997.
- Hoffman DA, Magee JC, Colbert CM, Johnston D. K<sup>+</sup> channel regulation of signal propagation in dendrites of hippocampal pyramidal neurons. *Nature* 387: 869–875, 1997.
- Hutcheon B, Fritschy JM, Poulter MO. Organization of GABA receptor alpha-subunit clustering in the developing rat neocortex and hippocampus. *Eur J Neurosci* 19: 2475–2487, 2004.
- Jones OT, Bernstein GM, Jones EJ, Jugloff DG, Law M, Wong W, Mills LR. N-Type calcium channels in the developing rat hippocampus: subunit, complex, and regional expression. *J Neurosci* 17: 6152–6164, 1997.

- Kampa BM, Letzkus JJ, Stuart GJ. Dendritic mechanisms controlling spike-timing-dependent synaptic plasticity. *Trends Neurosci* 30: 456–463, 2007.
- Klausberger T. GABAergic interneurons targeting dendrites of pyramidal cells in the CA1 area of the hippocampus. *Eur J Neurosci* 30: 947–957, 2009.
- Kramer AA, Ingraham NE, Sharpe EJ, Mynlieff M. Levels of Ca(V)1.2 L-type Ca(2+) channels peak in the first two weeks in rat hippocampus whereas Ca(V)1.3 channels steadily increase through development. *J Signal Transduct* 2012: 597214, 2012.
- Kwag J, Paulsen O. Bidirectional control of spike timing by GABA(A) receptor-mediated inhibition during theta oscillation in CA1 pyramidal neurons. *Neuroreport* 20: 1209–1213, 2009.
- Lee D, Lin BJ, Lee AK. Hippocampal place fields emerge upon single-cell manipulation of excitability during behavior. *Science* 337: 849–853, 2012.
- Leung LS, Peloquin P. GABA-B receptors inhibit backpropagating dendritic spikes in hippocampal CA1 pyramidal cells in vivo. *Hippocampus* 16: 388–407, 2006.
- Liu G. Local structural balance and functional interaction of excitatory and inhibitory synapses in hippocampal dendrites. *Nat Neurosci* 7: 373–379, 2004.
- Lohmann C, Kessels HW. The developmental stages of synaptic plasticity. *J Physiol* 592: 13–31, 2014.
- Lovett-Barron M, Turi GF, Kaifosh P, Lee PH, Bolze F, Sun XH, Nicoud JF, Zemelman BV, Sternson SM, Losonczy A. Regulation of neuronal input transformations by tunable dendritic inhibition. *Nat Neurosci* 15: 423–430, S421–S423, 2012.
- Luchkina NV, Huupponen J, Clarke VR, Coleman SK, Keinänen K, Taira T, Lauri SE. Developmental switch in the kinase dependency of long-term potentiation depends on expression of GluA4 subunit-containing AMPA receptors. *Proc Natl Acad Sci U S A* 111: 4321–4326, 2014.
- Lund JS, Griffiths S, Rumberger A, Levitt JB. Inhibitory synapse cover on the somata of excitatory neurons in macaque monkey visual cortex. *Cereb Cortex* 11: 783–795, 2001.
- Magee J, Hoffman D, Colbert C, Johnston D. Electrical and calcium signaling in dendrites of hippocampal pyramidal neurons. *Annu Rev Physiol* 60: 327–346, 1998.
- Magee JC. Dendritic hyperpolarization-activated currents modify the integrative properties of hippocampal CA1 pyramidal neurons. *J Neurosci* 18: 7613–7624, 1998.
- Maletic-Savatic M, Lenn NJ, Trimmer JS. Differential spatiotemporal expression of K<sup>+</sup> channel polypeptides in rat hippocampal neurons developing in situ and in vitro. *J Neurosci* 15: 3840–3851, 1995.
- Mann EO, Paulsen O. Role of GABAergic inhibition in hippocampal network oscillations. *Trends Neurosci* 30: 343–349, 2007.
- Martin LJ, Zurek AA, MacDonald JF, Roder JC, Jackson MF, Orser BA.  $\alpha$ 5GABAA receptor activity sets the threshold for long-term potentiation and constrains hippocampus-dependent memory. *J Neurosci* 30: 5269–5282, 2010.
- Marty S, Wehrle R, Alvarez-Leefmans FJ, Gasnier B, Sotelo C. Postnatal maturation of Na<sup>+</sup>, K<sup>+</sup>, 2Cl<sup>−</sup> cotransporter expression and inhibitory synaptogenesis in the rat hippocampus: an immunocytochemical analysis. *Eur J Neurosci* 15: 233–245, 2002.
- Megias M, Emri Z, Freund TF, Gulyas AI. Total number and distribution of inhibitory and excitatory synapses on hippocampal CA1 pyramidal cells. *Neuroscience* 102: 527–540, 2001.
- Meredith RM, Floyer-Lea AM, Paulsen O. Maturation of long-term potentiation induction rules in rodent hippocampus: role of GABAergic inhibition. *J Neurosci* 23: 11142–11146, 2003.
- Meredith RM, Holmgren CD, Weidum M, Burnashev N, Mansvelder HD. Increased threshold for spike-timing-dependent plasticity is caused by unreliable calcium signaling in mice lacking fragile X gene FMR1. *Neuron* 54: 627–638, 2007.
- Migliore M, Ferrante M, Ascoli GA. Signal propagation in oblique dendrites of CA1 pyramidal cells. *J Neurophysiol* 94: 4145–4155, 2005.
- Mody I. Aspects of the homeostatic plasticity of GABAA receptor-mediated inhibition. *J Physiol* 562: 37–46, 2005.
- Moser EI, Kropff E, Moser MB. Place cells, grid cells, and the brain's spatial representation system. *Annu Rev Neurosci* 31: 69–89, 2008.
- Nestor M, Hoffman D. Aberrant dendritic excitability: a common pathophysiology in CNS disorders affecting memory? *Mol Neurobiol* 45: 478–487, 2012a.
- Nestor MW, Hoffman DA. Differential cycling rates of Kv4.2 channels in proximal and distal dendrites of hippocampal CA1 pyramidal neurons. *Hippocampus* 22: 969–980, 2012b.
- Olmos-Serrano JL, Paluszkievicz SM, Martin BS, Kaufmann WE, Corbin JG, Huntsman MM. Defective GABAergic neurotransmission and pharmacological rescue of neuronal hyperexcitability in the amygdala in a mouse model of fragile X syndrome. *J Neurosci* 30: 9929–9938, 2010.
- Olsen RW, Sieghart W. GABA A receptors: subtypes provide diversity of function and pharmacology. *Neuropharmacology* 56: 141–148, 2009.
- Palmer MJ, Isaac JT, Collingridge GL. Multiple, developmentally regulated expression mechanisms of long-term potentiation at CA1 synapses. *J Neurosci* 24: 4903–4911, 2004.
- Pavlov I, Savchenko LP, Kullmann DM, Semyanov A, Walker MC. Outwardly rectifying tonically active GABAA receptors in pyramidal cells modulate neuronal offset, not gain. *J Neurosci* 29: 15341–15350, 2009.
- Pike FG, Meredith RM, Olding AW, Paulsen O. Rapid report: postsynaptic bursting is essential for “Hebbian” induction of associative long-term potentiation at excitatory synapses in rat hippocampus. *J Physiol* 518: 571–576, 1999.
- Poirazi P, Brannon T, Mel BW. Arithmetic of subthreshold synaptic summation in a model CA1 pyramidal cell. *Neuron* 37: 977–987, 2003.
- Ramos B, Lopez-Tellez JF, Vela J, Baglietto-Vargas D, del Rio JC, Ruano D, Gutierrez A, Vitorica J. Expression of alpha 5 GABAA receptor subunit in developing rat hippocampus. *Brain Res Dev Brain Res* 151: 87–98, 2004.
- Ross WN. Understanding calcium waves and sparks in central neurons. *Nat Rev Neurosci* 13: 157–168, 2012.
- Royer S, Zemelman BV, Losonczy A, Kim J, Chance F, Magee JC, Buzsaki G. Control of timing, rate and bursts of hippocampal place cells by dendritic and somatic inhibition. *Nat Neurosci* 15: 769–775, 2012.
- Scimemi A, Semyanov A, Sperk G, Kullmann DM, Walker MC. Multiple and plastic receptors mediate tonic GABAA receptor currents in the hippocampus. *J Neurosci* 25: 10016–10024, 2005.
- Shen H, Sabaliauskas N, Sherpa A, Fenton AA, Stelzer A, Aoki C, Smith SS. A critical role for alpha4betadelta GABAA receptors in shaping learning deficits at puberty in mice. *Science* 327: 1515–1518, 2010.
- Sjostrom PJ, Rancz EA, Roth A, Hausser M. Dendritic excitability and synaptic plasticity. *Physiol Rev* 88: 769–840, 2008.
- Sperk G, Schwarzer C, Tsunashima K, Fuchs K, Sieghart W. GABA(A) receptor subunits in the rat hippocampus I: immunocytochemical distribution of 13 subunits. *Neuroscience* 80: 987–1000, 1997.
- Stell BM, Mody I. Receptors with different affinities mediate phasic and tonic GABA(A) conductances in hippocampal neurons. *J Neurosci* 22: RC223, 2002.
- Sterratt DC, Groen MR, Meredith RM, van Ooyen A. Spine calcium transients induced by synaptically-evoked action potentials can predict synapse location and establish synaptic democracy. *PLoS Comput Biol* 8: e1002545, 2012.
- Tsubokawa H, Ross WN. IPSPs modulate spike backpropagation and associated [Ca<sup>2+</sup>]<sub>i</sub> changes in the dendrites of hippocampal CA1 pyramidal neurons. *J Neurophysiol* 76: 2896–2906, 1996.
- van Elburg RA, van Ooyen A. Impact of dendritic size and dendritic topology on burst firing in pyramidal cells. *PLoS Comput Biol* 6: e1000781, 2010.
- van Strien NM, Cappaert NL, Witter MP. The anatomy of memory: an interactive overview of the parahippocampal-hippocampal network. *Nat Rev Neurosci* 10: 272–282, 2009.
- Vasilyev DV, Barish ME. Postnatal development of the hyperpolarization-activated excitatory current Ih in mouse hippocampal pyramidal neurons. *J Neurosci* 22: 8992–9004, 2002.
- Vetter P, Roth A, Hausser M. Propagation of action potentials in dendrites depends on dendritic morphology. *J Neurophysiol* 85: 926–937, 2001.
- Williams SR, Mitchell SJ. Direct measurement of somatic voltage clamp errors in central neurons. *Nat Neurosci* 11: 790–798, 2008.
- Yang S, Su W, Bao S. Long-term, but not transient, threshold shifts alter the morphology and increase the excitability of cortical pyramidal neurons. *J Neurophysiol* 108: 1567–1574, 2012.
- Yasuda H, Barth AL, Stellwagen D, Malenka RC. A developmental switch in the signaling cascades for LTP induction. *Nat Neurosci* 6: 15–16, 2003.
- Zhang ZW. Maturation of layer V pyramidal neurons in the rat prefrontal cortex: intrinsic properties and synaptic function. *J Neurophysiol* 91: 1171–1182, 2004.